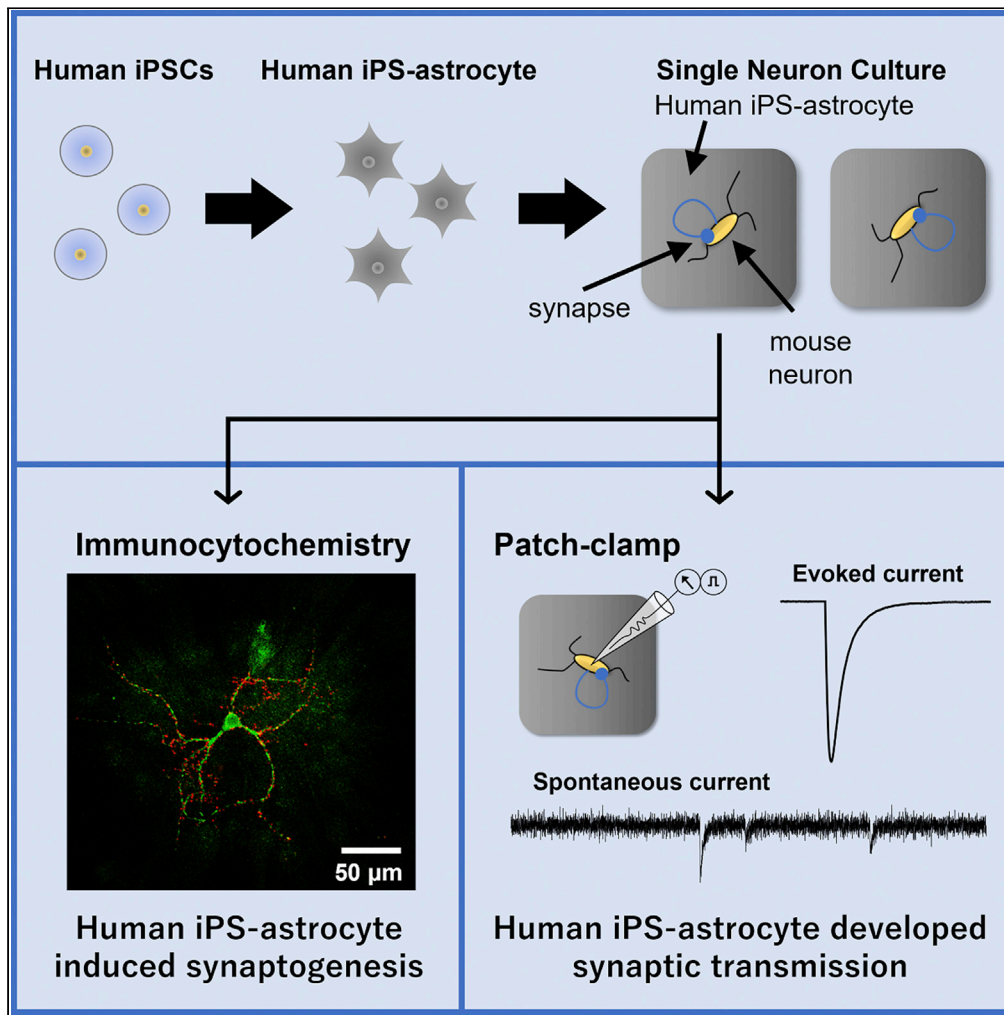


Article

Establishment of autaptic culture with human-induced pluripotent stem cell-derived astrocytes



Kouya Uchino,
Yasuyoshi Tanaka,
Sayaka Kawaguchi, ...,
Shutaro Katsurabayashi,
Shinichi Hirose,
Katsunori Iwasaki

shutarok@fukuoka-u.ac.jp

Highlights

We developed an autaptic culture with human iPSCs-derived astrocytes

Neurons in HiAAs developed after culture and formed functional synapses

EPSC and mEPSC were recorded showing HiAs promoted synapse formation/maturation

Autaptic cultures can be used to analyze synaptic activity and human CNS disease

Uchino et al., iScience 25, 104762
August 19, 2022 © 2022 The Author(s).
<https://doi.org/10.1016/j.isci.2022.104762>



Article

Establishment of autaptic culture with human-induced pluripotent stem cell-derived astrocytes

Kouya Uchino,¹ Yasuyoshi Tanaka,^{2,3,4} Sayaka Kawaguchi,¹ Kaori Kubota,¹ Takuya Watanabe,¹ Shutaro Katsurabayashi,^{1,4,6,*} Shinichi Hirose,^{3,4,5} and Katsunori Iwasaki¹

SUMMARY

Although astrocytes are involved in the pathogenesis of CNS diseases, how they induce synaptic abnormalities is unclear. Currently, *in vitro* pathological astrocyte cultures or animal models do not reproduce human disease phenotypes accurately. Induced pluripotent stem cells (iPSCs) are replacing animal models in pathological studies. We developed an autaptic culture (AC) system containing single neuron cultures grown on microislands of astrocytes. AC with human iPSC-derived astrocytes (HiA) was established. We evaluated the effect of astrocytes on the synaptic functions of human-derived neurons. We found a significantly higher Na⁺ current amplitude, membrane capacitance, and number of synapses, as well as longer dendrites, in HiAACs compared with neuron monocultures. Furthermore, HiAs were involved in the formation and maturation of functional synapses that exhibited excitatory postsynaptic currents. This system can facilitate the study of CNS diseases and advance the development of drugs targeting glial cells.

INTRODUCTION

Brain cells are composed of neurons and glial cells. Astrocytes are a type of glial cell involved in synaptic transmission and the formation and maturation of synapses; thus, they are a constitutive element of the tripartite synapse (Allen and Barres, 2009; Eroglu and Barres, 2010; Perea et al., 2009). Additionally, astrocytes contribute to the pathogenesis of multiple CNS diseases such as Alzheimer's disease, Parkinson's disease, autism, and epilepsy (Cai et al., 2017; Booth et al., 2017; Petrelli et al., 2016; Patel et al., 2019). Therefore, astrocytes are attracting attention as a therapeutic drug target for these diseases. However, a detailed analysis of synaptic modification by pathological astrocytes is limited by a lack of models that represent synaptic abnormalities caused by pathological astrocytes in humans and the inability of animal models to faithfully reproduce human disease phenotypes.

The establishment of induced pluripotent stem cells (iPSCs) allows the differentiation of stem cells into various types of cells while preserving their genotype. Therefore, patient iPSCs are replacing animal models in pathological analysis and drug discovery. Technological advances have provided access to human astrocytes through the induction of iPSCs and the mRNA profiles, protein expressions, and morphology of iPSC-derived astrocytes (HiAs) have been reported (Roybon et al., 2013; Santos et al., 2017; Tcw et al., 2017; Perriot et al., 2018; Lundin et al., 2018; Canals et al., 2018). Recently, astrocytes were established from the iPSCs of patients with several CNS diseases, and their role in pathogenesis was analyzed (Suga et al., 2019). Furthermore, neurons co-cultured with pathological astrocytes have been used to study their morphology, synaptic gene expression, protein levels, and spontaneous synaptic responses (Williams et al., 2014; Russo et al., 2018). However, these studies did not investigate detailed synaptic functions such as synaptic transmission evoked by electrical stimulation and morphological analysis at the single neuron level.

Therefore, we focused on autaptic cultures, single neuron cultures grown in isolation on microislands of astrocytes that form synapses exclusively with themselves (Bekkers and Stevens, 1991; Bekkers, 2020). This system allows the analysis of the number of synapses in a single neuron, synaptic transmission, and the morphology of dendrites and axons (Kawano et al., 2012). Furthermore, synaptic vesicle pool size

¹Department of Neuropharmacology, Faculty of Pharmaceutical Sciences, Fukuoka University, 8-19-1 Nanakuma, Jonan-ku, Fukuoka 814-0180, Japan

²Department of Advanced Pharmacology, Daiichi University of Pharmacy, 22-1 Tamagawa-machi, Minami-ku, Fukuoka 815-8511, Japan

³IONtarget, Co., Inc., 1-3-70-5805 Momochihama, Sawaraku, Fukuoka 814-0006, Japan

⁴Research Institute for the Molecular Pathogenesis of Epilepsy, Fukuoka University, 7-45-1 Nanakuma, Jonan-ku, Fukuoka 814-0180, Japan

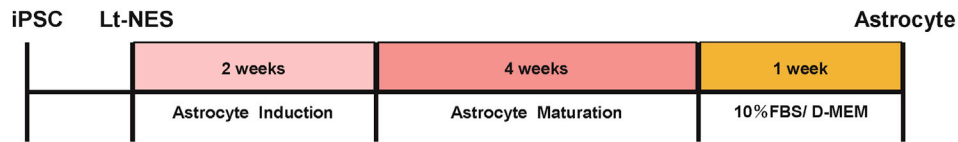
⁵General Medical Research Center, School of Medicine, Fukuoka University, 7-45-1 Nanakuma, Jonan-ku, Fukuoka 814-0180, Japan

⁶Lead contact

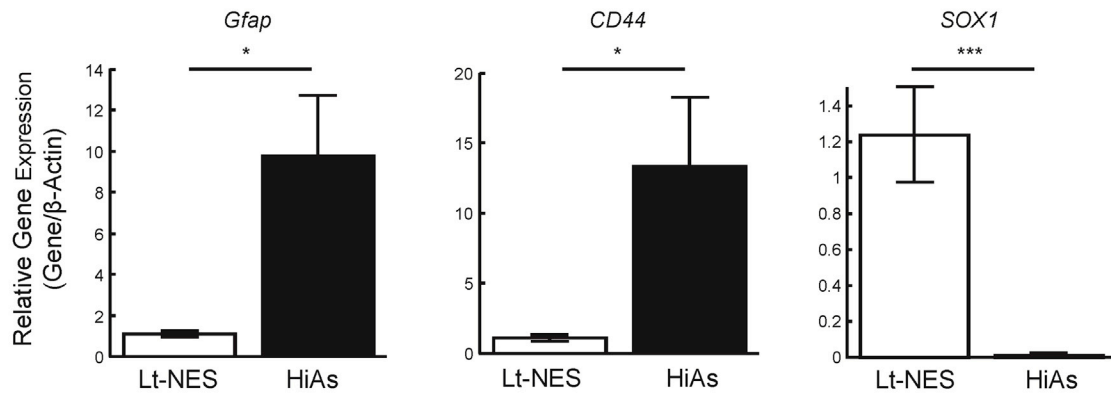
*Correspondence: shutarok@fukuoka-u.ac.jp
<https://doi.org/10.1016/j.isci.2022.104762>



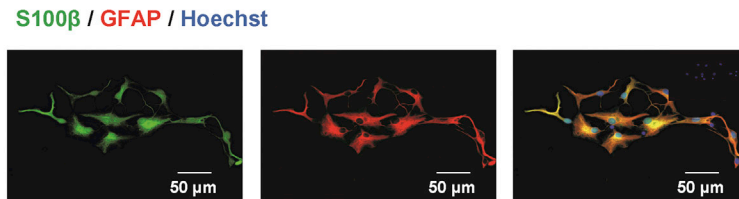
A



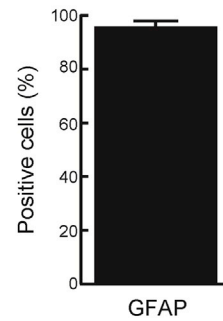
B



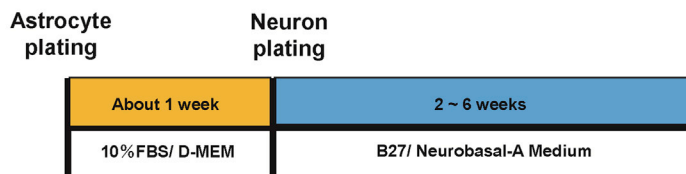
C



D



E



F

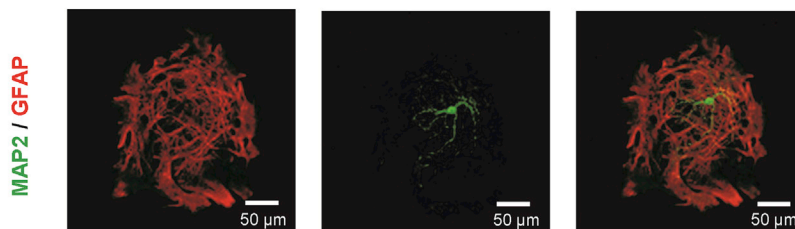


Figure 1. Establishment of an autaptic culture with human iPSC-derived astrocytes

- (A) The protocol for the generation of human iPSC-derived astrocytes (HiAs).
(B) mRNA levels of *glial fibrillary acidic protein (Gfap)*, *CD44*, and *SOX1* in Lt-NES cells or HiAs (n = number of cultures: Lt-NES cells, n = 8; HiAs, n = 8; two experiments). Data are represented as mean \pm SEM (Student's t test, *p < 0.05, ***p < 0.001).
(C) Representative images of HiAs immunostained for GFAP (red) and S100 β (green). Scale bar 50 μ m.
(D) Percentage of GFAP-positive cells in HiAs (n = number of cultures: n = 7; two experiments). Data are represented as mean \pm SEM.
(E) The protocol of the autaptic culture with HiAs (HiAACs).
(F) Representative images of HiAACs immunostained for GFAP (red) and microtubule-associated protein 2 (MAP2; green). Scale bar 50 μ m.

and vesicular release probability can be assessed (Pyotte and Rosenmund, 2002). Recently, three groups developed a protocol to generate autaptic cultures of iPSC-derived neurons (Meijer et al., 2019; Rhee et al., 2019; Fenske et al., 2019). In these cultures, neurons were differentiated from human iPSCs and co-cultured with astrocytes derived from the cortex of mice or rats. These cultures can be used as a model to evaluate synaptic functions specific to human-derived neurons. To investigate the involvement of astrocytes in synaptic activity and CNS disease, we established autaptic cultures with human iPSCs-derived astrocytes (HiAs Autaptic Cultures, HiAACs).

RESULTS**Establishment of an autaptic culture with human iPSCs-derived astrocytes**

We differentiated human iPSCs into astrocytes as previously reported (Perriot et al., 2018). First, we differentiated human iPSCs into long-term self-renewing neuroepithelial-like stem cells (Lt-NES cells) (Falk et al., 2012). As shown in Figure S1, after the isolation of rosette cells, the expressions of the neuronal progenitor marker Nestin and neuronal rosette maker DACH1 were observed by immunostaining Lt-NES cells. Then, we differentiated Lt-NES cells to astrocytes for 6 weeks (Figure 1A). After 6 weeks, the cells were cultured in medium with 10% fetal bovine serum (FBS) for 1 week and reacted with mitomycin C for 2 h to stop cell proliferation. To confirm that the differentiated cells had become astrocytes, we analyzed the mRNA levels of *glial fibrillary acidic protein (Gfap)* and *CD44*, which are astrocyte markers, and *SOX1*, a marker of neural stem cells. HiAs had high expressions of *Gfap* and *CD44*, and a low expression of *SOX1* (Figure 1B). Immunocytochemistry showed HiAs were positive for GFAP and S100 β , markers of astrocytes, and that more than 90% of cells were positive for GFAP (Figure 1C and 1D). HiAACs were prepared based on mouse autaptic cultures as reported previously (Kawano et al., 2012, 2017; Oyabu et al., 2019, 2020; Takeda et al., 2021; Katsurabayashi et al., 2021; Uchino et al., 2021). HiAs were plated onto microdot-coated coverslips. Approximately 1 week later, we confirmed the HiAs formed microislands and then co-cultured them with hippocampal neurons from ICR mice (Figure 1E). Immunocytochemical staining with microtubule-associated protein 2 (MAP2) and GFAP confirmed the presence of single neurons grown on HiAs (Figure 1F).

Neurons in HiAACs form functional synapses

Astrocytes promote the development of neurons and synaptic formation by diffusible factors and adhesion factors (Hama et al., 2004; Allen and Barres, 2009). Therefore, we measured neural function between HiAACs and neuron monocultures (NMCs) by patch-clamp recording to investigate whether HiAs are involved in neuronal development. The experiment was performed on neurons cultured for 2–3 weeks. We analyzed the amplitude of voltage-dependent Na⁺ current components, which underlie action potentials evoked by electrical stimulation under the voltage-clamp mode. The amplitude of Na⁺ currents was significantly higher in the HiAACs compared with NMCs (Figure 2A and 2B). Next, we examined the membrane capacitance between HiAACs and NMCs. The membrane capacitance increases in proportion to the size of the soma. The mean membrane capacitance was significantly higher in the HiAACs than in the NMCs (Figure 2C). In contrast, the Na⁺ current density (nA/pF), calculated by dividing the Na⁺ current amplitude by the membrane capacitance, was not significantly different between HiAACs and NMCs (Figure 2D). Next, we measured the excitatory postsynaptic current (EPSC) and miniature EPSC (mEPSC) to determine whether HiAs were involved in the formation and maturation of synapses. The recorded EPSC was mostly blocked by CNQX (5 μ M), a competitive antagonist of AMPA-subtype of ionotropic glutamate receptors, but not by AP5 (15 μ M), a competitive antagonist of the NMDA-subtype of ionotropic glutamate receptors (Figures S2A and S2B). Consequently, the recorded EPSCs showed AMPA receptor-mediated EPSCs. Glutamate receptors are classified into two types, namely, AMPA and NMDA receptors. NMDA receptors are usually blocked by Mg²⁺, but they can be pharmacologically activated by Mg²⁺-free extracellular solution containing 10 μ M glycine (Rosenmund et al., 1993; Hessler et al., 1993). Therefore, we confirmed whether EPSCs exhibited AMPA and NMDA components in HiAACs. We observed that

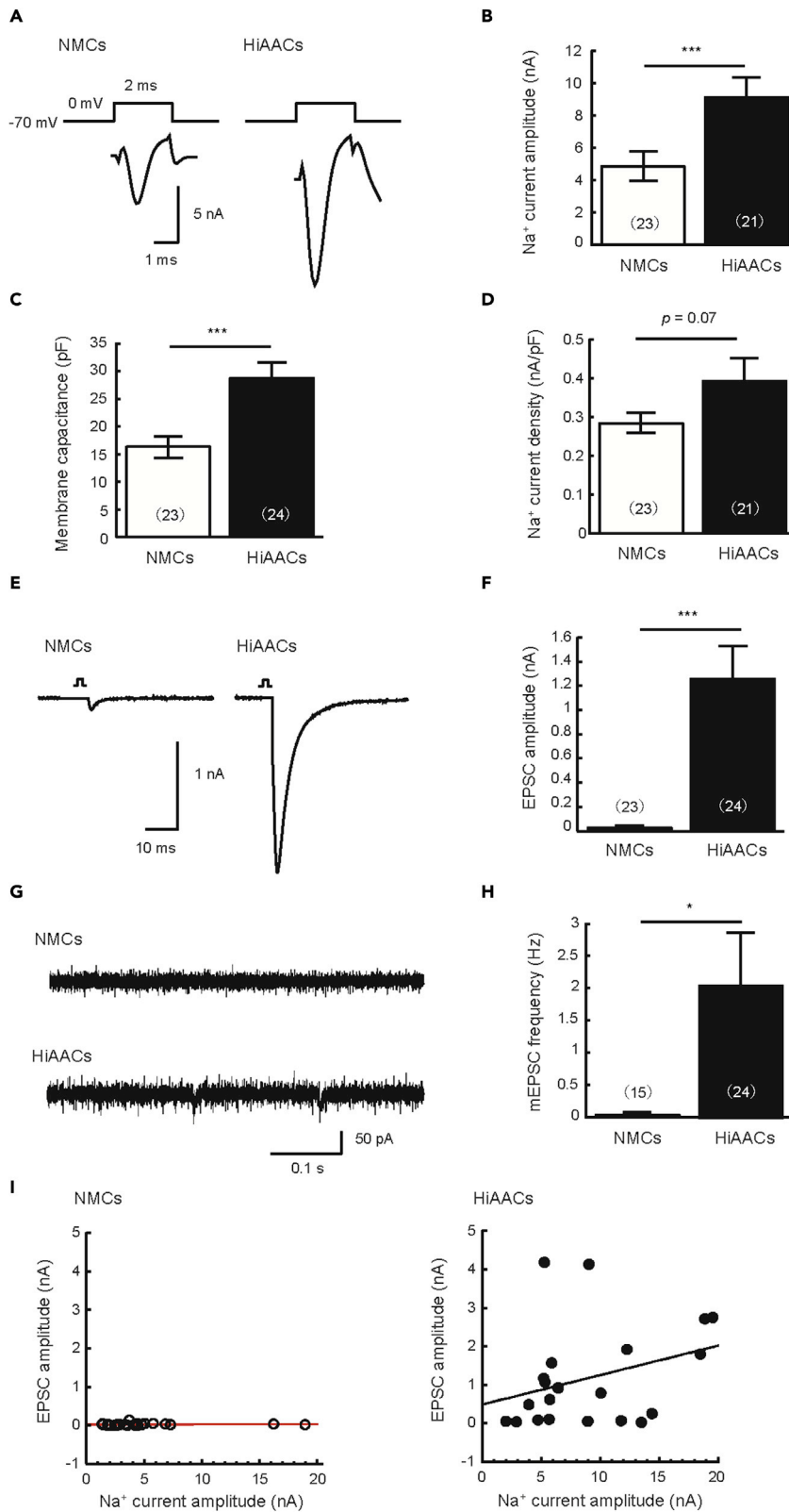


Figure 2. Neurons in HiAAs form functional synapses

- (A) Representative traces of voltage-dependent Na⁺ currents recorded by voltage-clamp from single neurons in NMC or HiAAC.
- (B) Mean amplitudes of Na⁺ currents in single neurons in NMC or HiAAC (n = number of neurons: NMCs, n = 23; HiAAs, n = 21; three cultures).
- (C) Mean membrane capacitance in single neurons in NMC or HiAAC (n = number of neurons: NMCs, n = 23; HiAAs, n = 24; three cultures).
- (D) Mean Na⁺ current density in single neurons in NMC or HiAAC (n = number of neurons: NMCs, n = 23; HiAAs, n = 21; three cultures).
- (E) Representative traces of evoked excitatory postsynaptic currents (EPSCs) recorded from single neurons in NMC or HiAAC. Depolarization artifacts caused by the generated action currents were removed for clarity.
- (F) Mean amplitudes of evoked EPSCs in single neurons in NMC or HiAAC (n = number of neurons: NMCs, n = 23; HiAAs, n = 24; three cultures).
- (G) Representative miniature EPSC (mEPSC) traces in single neurons in NMC or HiAAC.
- (H) Mean mEPSC frequencies in single neurons in NMC or HiAAC (n = number of neurons: NMCs, n = 15; HiAAs, n = 24; three cultures).
- (I) Correlation between Na⁺ current and EPSC in HiAAs (left) and NMCs (right). The x axis is the Na⁺ current amplitude and the y axis is the EPSC amplitude (n = number of neurons: NMCs, n = 23; HiAAs, n = 21; three cultures). All data are represented as mean ± SEM (Student's t test, *p < 0.05, ***p < 0.001).

EPSCs exhibited AMPA receptor-mediated fast decay and NMDA receptor-mediated slow decay components in the Mg²⁺-free extracellular solution containing 10 μM glycine (Figure S2C and S2D). Indeed, the recorded EPSCs were divided into an AMPA receptor-mediated component blocked by CNQX (5 μM) and an NMDA receptor-mediated component blocked by AP5 (15 μM). These results are consistent with the characteristics of excitatory synaptic transmission in mouse autaptic cultures as reported previously (Kawano et al., 2012). In contrast to the extremely small EPSCs measured by NMCs, the EPSCs measured by HiAAs were sufficiently large (Figure 2E and 2F). mEPSCs were observed in HiAAs whereas almost no mEPSCs were observed in NMCs (Figure 2G and 2H). Furthermore, there was a proportional increase in EPSCs with increasing Na⁺ currents in HiAAs (Figure 2I). These results indicate that neurons in HiAAs develop by co-culture with HiAs and form functional synapses that exhibit EPSCs and mEPSCs.

Neurons in HiAAs develop morphologically and form excitatory synapses

The development of synaptic function in HiAAs (Figure 2) suggested that dendrites may be longer with a higher number of synapses when compared with NMCs. We measured the numbers of excitatory synapses in NMC and HiAAC neurons by immunostaining for vesicular glutamate transporter 1, a glutamatergic pre-synaptic protein. HiAAs formed more than 100 excitatory synapses compared with almost no excitatory synapses in NMCs (Figure 3A and 3B). Next, we analyzed the length and number of branches of dendrites in neurons labeled by MAP2. Dendritic length was significantly longer and the number of branches of neurons was significantly higher in HiAAs than in NMCs (Figure 3A, 3C, and 3D). Furthermore, there was a proportional increase in the number of excitatory synapses with increasing dendritic length in HiAAs (Figure 3E). These results indicate that HiAAC neurons develop morphologically and form excitatory synapses by co-culture with HiAs.

HiAAs mature 2 to 4 weeks after culture and can still be used after 6 weeks *in vitro*

To investigate the maturation period of HiAAs, we measured synaptic transmission in neurons cultured for 2, 4, and 6 weeks *in vitro* (WIV). The evoked EPSC amplitude was significantly higher in WIV4 than in WIV2, whereas it was similar between WIV4 and WIV6 (Figure 4A and 4B). The mEPSC amplitude was also significantly higher in WIV4 than in WIV2, whereas it was similar between WIV4 and WIV6 (Figure 4C and 4D). Although the mEPSC frequency tended to be higher between WIV2 and WIV4, the change was not statistically significant (Figure 4C and 4E). Finally, we measured the numbers of excitatory synapses in single neurons in WIV2, WIV4, and WIV6 (Figure 4F and 4G). The numbers of excitatory synapses were significantly higher in WIV4 than in WIV2, whereas they were similar between WIV4 and WIV6.

DISCUSSION

Here, we established an autaptic culture with HiAs. HiAAs matured 2 to 4 weeks after culture and could still be used after 6 weeks *in vitro* (Figures 4 and S3). This methodology can be used to analyze the number of synapses and morphology of single neurons co-cultured with human iPS cell-derived astrocytes, and to record evoked synaptic transmission. Previous studies have reported spontaneous synaptic responses as

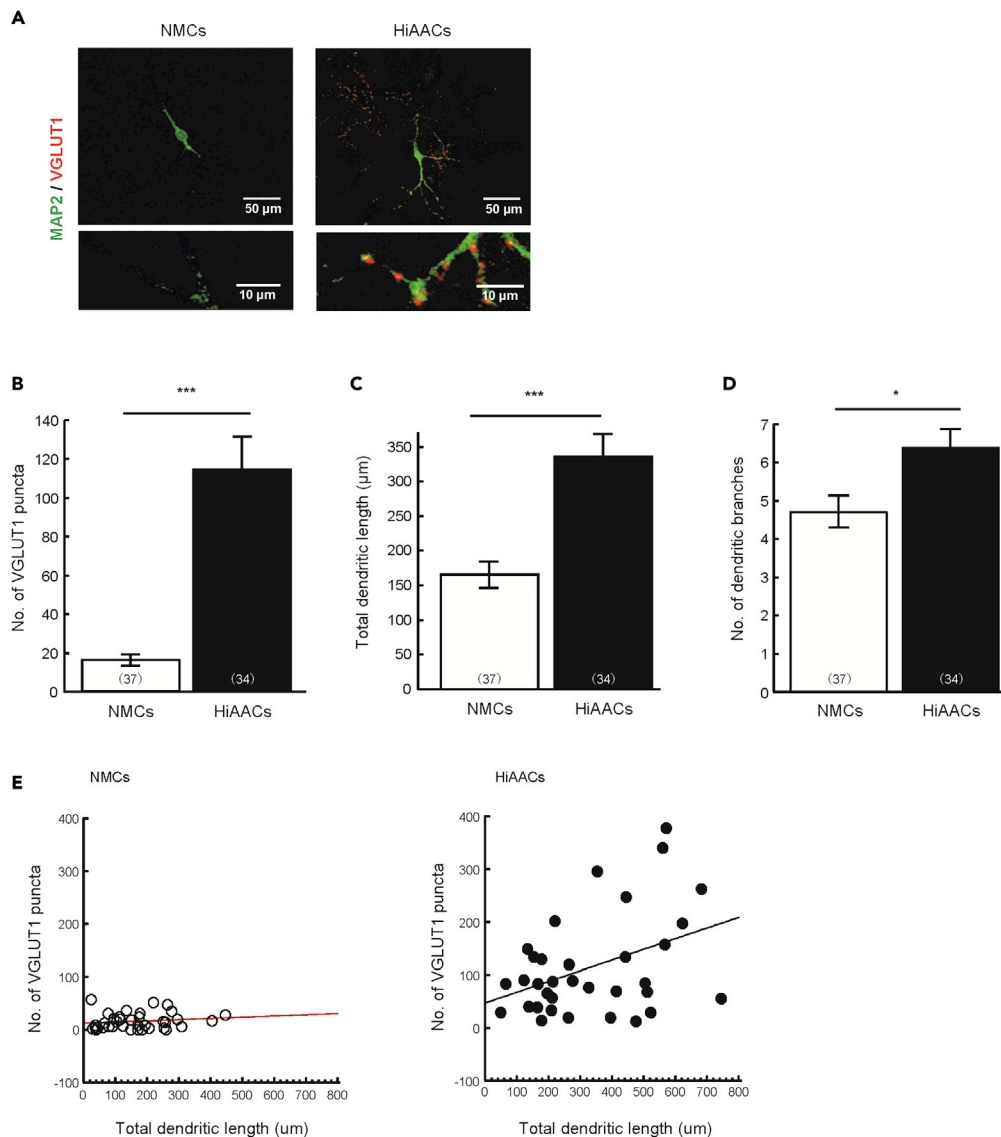


Figure 3. Neurons in HiAACs develop morphologically and form excitatory synapses

(A) Representative images of single neurons in NMC or HiAAC immunostained for vesicular glutamate transporter 1 (VGLUT1; red) and MAP2 (green). Parts of the top row (scale bar 50 μ m) are enlarged in the bottom row (scale bar 10 μ m). (B) Mean number of VGLUT1-positive synaptic puncta in single neurons in NMC or HiAAC. (C) Mean total dendritic length in single neurons in NMC or HiAAC. (D) Mean number of dendritic branches in single neurons in NMC or HiAAC. (E) Correlation between dendritic length and number of synapses in HiAACs (left) and NMCs (right). The x axis is the total dendritic length and the y axis is the number of VGLUT1-positive synaptic puncta. n = number of neurons: NMCs, n = 37; HiAACs, n = 34; two cultures. All data are represented as mean \pm SEM (Student's t test, *p < 0.05, ***p < 0.001).

evidence of synaptic function in neurons co-cultured with human astrocytes (Williams et al., 2014; Lischka et al., 2018; Canals et al., 2018; Tchiew et al., 2019; VanderWall et al., 2019; Hedegaard et al., 2020). However, we showed that spontaneous synaptic responses alone may be poor evidence of synaptic function, because in our study there was no change in mEPSC frequency despite an increase in evoked EPSC amplitude from WIV2 to WIV4. Therefore, when studying synaptic function, it is important to analyze spontaneous synaptic transmission as well as evoked synaptic transmission. Additionally, although not examined in the present study, HiAACs can be used to assess parameters such as synaptic vesicle pool size and vesicular release probability. Therefore, the methodology presented here will facilitate the study of tripartite synapses with a focus on astrocytes.

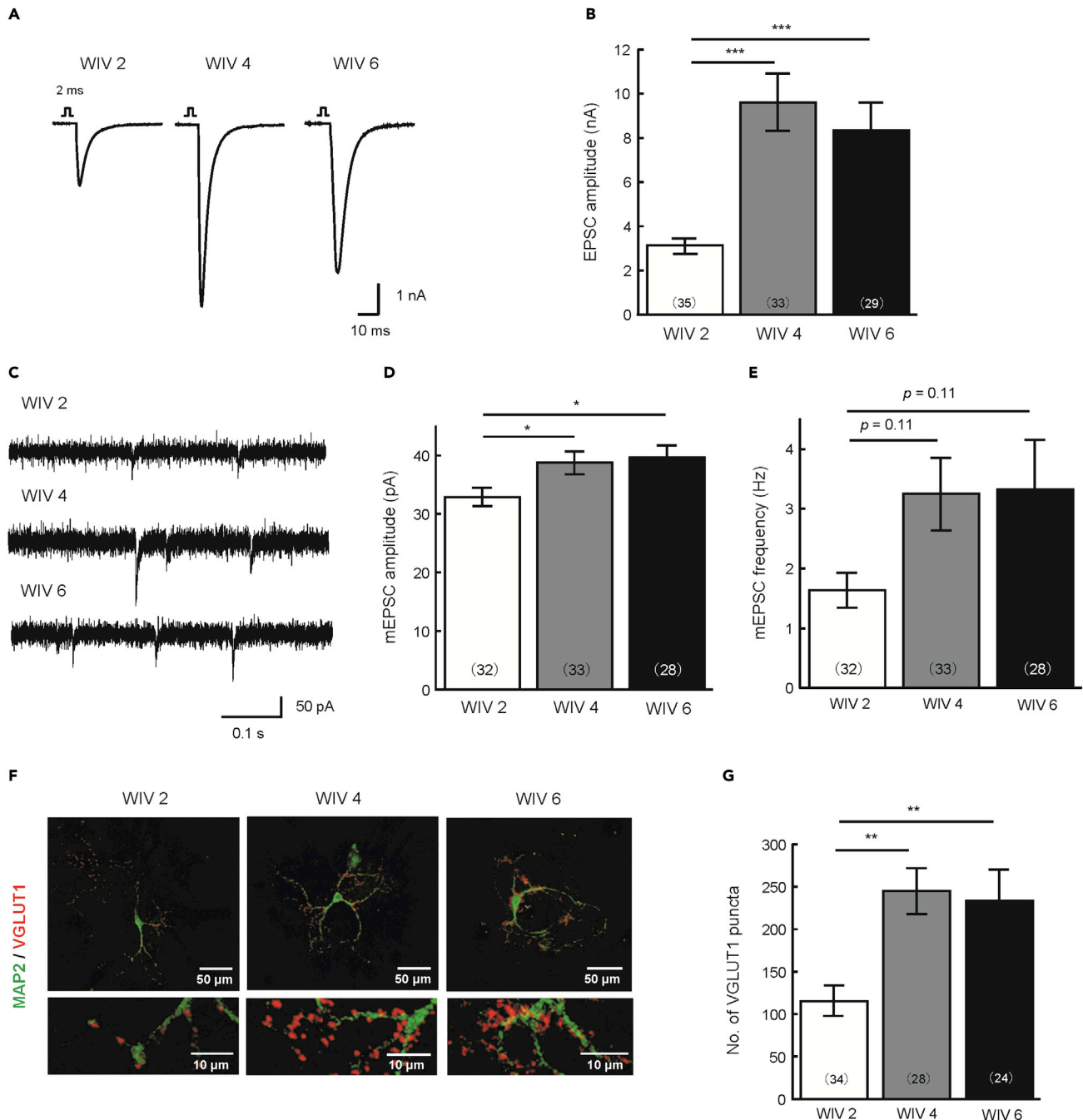


Figure 4. HiAACs mature from 2 to 4 weeks in culture and can be used for experiments for at least 6 weeks *in vitro*

(A) Representative traces of evoked EPSCs recorded from HiAACs neurons cultured for 2, 4, or 6 weeks (WIV2, WIV4, and WIV6) by the time of electrophysiological recording.

(B) Mean amplitudes of the evoked EPSCs in HiAAC neurons of WIV2, WIV4, and WIV6 (n = number of neurons: WIV2, n = 35; WIV4, n = 33; WIV6, n = 29; four cultures).

(C) Representative mEPSC traces in HiAAC neurons of WIV2, WIV4, and WIV6.

(D and E) Mean mEPSC frequencies and amplitudes in HiAAC neurons of WIV2, WIV4, and WIV6 (n = number of neurons: WIV2, n = 32; WIV4, n = 33; WIV6, n = 28; four cultures).

(F) Representative images of HiAAC neurons of WIV2, WIV4, or WIV6 immunostained for the dendritic marker MAP2 (green) and the excitatory nerve terminal marker VGLUT1 (red). Parts of the top row (scale bar 50 μ m) are enlarged in the bottom row (scale bar 10 μ m).

(G) Mean number of VGLUT1-positive synaptic puncta in HiAAC neurons of WIV2, WIV4, and WIV6 (n = number of neurons: WIV2, n = 34; WIV4, n = 28; WIV6, n = 24; two cultures). All data are represented as mean \pm SEM (Tukey's t test, *p < 0.05, **p < 0.01, ***p < 0.001).

The astrocytes used in this study were isolated at high purity and expressed markers for astrocytes at the gene and protein levels. We produced HiAAs by culturing HiAs in serum-containing medium to form microislands (Figure 1E). Serum-containing medium is used for primary astrocyte cultures (McCarthy and de Vellis, 1980) and is also frequently used for other HiA cultures (Roybon et al., 2013; Santos et al., 2017; Tcw et al., 2017). However, serum induces some features of reactive astrocytes (Zamanian et al., 2012; Zhang et al., 2016; Perriot et al., 2018). These reports suggested that using astrocytes cultured with serum to investigate the pathogenesis of patient-derived astrocytes might bias the results. However, the activation of astrocytes is associated with some CNS diseases; therefore, it is better to use reactive astrocytes to analyze the pathogenesis of such diseases (Roybon et al., 2013; Santos et al., 2017). As described above, there are many methods of astrocyte differentiation, each with different characteristics. Therefore, it is important to choose the appropriate astrocyte differentiation method required for specific purposes.

Much of our understanding of the physiology of astrocytes in disease, including our study, is almost entirely restricted to observations in murine models (Kawano et al., 2017; Takeda et al., 2021; Cai et al., 2017; Booth et al., 2017; Petrelli et al., 2016; Patel et al., 2019). However, human astrocytes are larger and more complex than mouse astrocytes (Oberheim et al., 2006, 2009). In addition, human and mouse astrocytes respond differently to extracellular glutamate (Zhang et al., 2016). Therefore, human astrocytes may have different roles in synaptic activity compared with mouse astrocytes. Indeed, drugs that showed promising results in animal models have failed in human trials (Cavanaugh et al., 2014; Cummings et al., 2014; Rothstein, 2003; Waldmeier et al., 2006), probably because of the inability of animal models to faithfully reproduce human disease phenotypes. The current study developed a more human-like *in vitro* model using mammalian-derived astrocytes instead of rodents. We plan to develop an entirely human-derived autaptic culture preparation by replacing single neurons with human iPSCs.

HiAAs formed functional synapses that exhibited EPSCs and mEPSCs. To culture single neurons, neurons must be cultured at a low density. However, primary neurons cannot grow at a low density and form mature synapses (Banker and Cowan, 1977; Brewer et al., 1994). However, astrocytes promote the synaptic maturation of neurons by diffusible factors and adhesion factors (Clarke and Barres, 2013; Allen and Eroglu, 2017). In this study, we used HiAs as feeder cells, which led to the formation of mature synapses and the recording of synaptic transmission in single neuron cultures. Therefore, in HiAAs, we expect that HiAs are involved in the maturation of neurons by the secretion of diffusible factors and expression of adhesion factors similar to that in mouse and rat astrocytes (Huettner and Baughman, 1986; Banker, 1980).

This study established a single neuron model co-cultured with human iPSC-derived astrocytes to advance research on synaptic modifications specific to human astrocytes. Using mouse autaptic cultures, we previously reported synaptic modification by pathological astrocytes in Alzheimer's disease and autism models (Kawano et al., 2017; Oyabu et al., 2019; Takeda et al., 2021). Therefore, autaptic cultures can be analyzed for synaptic modification by astrocytes of various phenotypes. Although we used healthy astrocytes in this study, HiAAs can be used to study various phenotypes by using patient-derived astrocytes. The establishment of this culture allows a detailed analysis of synaptic modification by patient-derived astrocytes. The methodology presented here should facilitate the study of tripartite synapses with a focus on human astrocytes.

Limitations of the study

We did not examine the phenotype of human iPSC-derived neurons co-cultured with HiAs. Nevertheless, the present model allowed the analysis of the effect of HiAs on synapse formation and function. In this study, only one iPSC line was used. For the *in vitro* studies using iPSC cells, it is important to perform experiments with multiple cell lines to ensure the reproducibility of the data. However, recent technological improvements in culture methods have made the accuracy of iPSC cells derived from healthy humans more uniform (Perriot et al., 2018; Lundin et al., 2018; Meijer et al., 2019; Rhee et al., 2019; Fenske et al., 2019; Leventoux et al., 2020). Therefore, we used only one cell line from healthy human-derived iPSC cells.

STAR★METHODS

Detailed methods are provided in the online version of this paper and include the following:

- KEY RESOURCES TABLE

- **RESOURCE AVAILABILITY**
 - Lead contact
 - Materials availability
 - Data and code availability
- **EXPERIMENTAL MODEL AND SUBJECT DETAILS**
 - Animals
 - iPSC line
- **METHOD DETAILS**
 - Establishing and maintaining Lt-NES cells derived from 201B7 iPSCs
 - Generation of HiAs
 - HiAAs and NMCs
 - Quantitative PCR
 - Purity of HiAs
 - Immunocytochemistry, image acquisition, and analysis
 - Electrophysiology
- **QUANTIFICATION AND STATISTICAL ANALYSIS**
 - Statistical analysis

SUPPLEMENTAL INFORMATION

Supplemental information can be found online at <https://doi.org/10.1016/j.isci.2022.104762>.

ACKNOWLEDGMENTS

This work was supported by funding from Fukuoka University (No. 217302) to S.K. (Shutaro Katsurabayashi), a KAKENHI Grant-in-Aid for Transformative Research Areas (B) to S.K. (Shutaro Katsurabayashi) (No. 21H05165), a KAKENHI Grant-in-Aid for Scientific Research (B) to S.K. (Shutaro Katsurabayashi) (No. 20H04506) and a KAKENHI Grant-in-Aid for Scientific Research (C) to Y.T. (No. 21K07784) from the Japan Society for the Promotion of Science, the Science Research Promotion Fund and The Fukuoka University Fund to S.H. (Nos. G19001 and G20001), a grant for a Practical Research Project for Rare/Intractable Diseases from the Japan Agency for Medical Research and development (AMED) to S.H. (Nos. 15ek0109038h0002 and 16ek0109038h0003), a KAKENHI Grant-in-Aid for Scientific Research (A) to S.H. (No. 15H02548), a KAKENHI Grant-in-Aid for Scientific Research (B) to S.H. (Nos. 20H03651, 20H03443, and 20H04506), the Acceleration Program for Intractable Diseases Research utilizing Disease-specific iPSC cells from AMED to S.H. (Nos. 17bm0804014h0001, 18bm0804014h0002, and 19bm0804014h0003), a Grant-in-Aid for Research on Measures for Intractable Diseases to S.H. (H31-Nanji-Ippan-010), Program for the Strategic Research Foundation at Private Universities 2013–2017 from the Ministry of Education, Culture, Sports, Science, and Technology (MEXT) to S.H. (No. 924), and Center for Clinical and Translational Research of Kyushu University Hospital to S.H. (No. 201m0203009j0004). We thank the members of our laboratory for their help. We also thank Bronwen Gardner, PhD, and J. Ludovic Croxford, PhD, from Edanz (<https://jp.edanz.com/ac>) for editing a draft of this manuscript.

AUTHOR CONTRIBUTIONS

K.U., Y.T., and S.K. (Sayaka Kawaguchi) performed experiments and analyzed data; S.K. (Shutaro Katsurabayashi) conceived the study; K.K., T.W., K.I., and S.H. interpreted the data; K.U. and S.K. (Shutaro Katsurabayashi) wrote the manuscript with input from all authors. All authors reviewed the manuscript.

DECLARATION OF INTERESTS

The authors declare no competing interests.

Received: January 6, 2022

Revised: May 25, 2022

Accepted: July 11, 2022

Published: August 19, 2022

REFERENCES

Allen, N.J., and Barres, B.A. (2009). Neuroscience: glia - more than just brain glue. *Nature* 457, 675–677. <https://doi.org/10.1038/457675a>.

Allen, N.J., and Eroglu, C. (2017). Cell biology of astrocyte-synapse interactions. *Neuron* 96, 697–708. <https://doi.org/10.1016/j.neuron.2017.09.056>.

Banker, G.A. (1980). Trophic interactions between astroglial cells and hippocampal neurons in culture. *Science* 209, 809–810. <https://doi.org/10.1126/science.7403847>.

Banker, G.A., and Cowan, W.M. (1977). Rat hippocampal neurons in dispersed cell culture. *Brain Res.* 126, 397–442. [https://doi.org/10.1016/0006-8993\(77\)90594-7](https://doi.org/10.1016/0006-8993(77)90594-7).

Bekkers, J.M. (2020). Autaptic cultures: methods and applications. *Front. Synaptic Neurosci.* 12, 18. <https://doi.org/10.3389/fnsyn.2020.00018>.

Bekkers, J.M., and Stevens, C.F. (1991). Excitatory and inhibitory autaptic currents in isolated hippocampal neurons maintained in cell culture. *Proc. Natl. Acad. Sci. USA* 88, 7834–7838. <https://doi.org/10.1073/pnas.88.17.7834>.

Booth, H.D.E., Hirst, W.D., and Wade-Martins, R. (2017). The role of astrocyte dysfunction in Parkinson's disease pathogenesis. *Trends Neurosci.* 40, 358–370. <https://doi.org/10.1016/j.tins.2017.04.001>.

Brewer, G.J., Torricelli, J., Evege, E.K., and Price, P.J. (1994). Neurobasal medium/B27 supplement: a new serum-free medium combination for survival of neurons. *Focus* 16, 6–9.

Cai, Z., Wan, C.Q., and Liu, Z. (2017). Astrocyte and Alzheimer's disease. *J. Neurol.* 264, 2068–2074. <https://doi.org/10.1007/s00415-017-8593-x>.

Canals, I., Ginisty, A., Quist, E., Timmerman, R., Fritze, J., Miskinyte, G., Monni, E., Hansen, M.G., Hidalgo, I., Bryder, D., et al. (2018). Rapid and efficient induction of functional astrocytes from human pluripotent stem cells. *Nat. Methods* 15, 693–696. <https://doi.org/10.1038/s41592-018-0103-2>.

Cavanaugh, S.E., Pippin, J.J., and Barnard, N.D. (2014). Animal models of Alzheimer disease: historical pitfalls and a path forward. *ALTEX* 31, 279–302. <https://doi.org/10.14573/altex.1310071>.

Clarke, L.E., and Barres, B.A. (2013). Emerging roles of astrocytes in neural circuit development. *Nat. Rev. Neurosci.* 14, 311–321. <https://doi.org/10.1038/nrn3484>.

Cummings, J.L., Morstorf, T., and Zhong, K. (2014). Alzheimer's disease drug-development pipeline: few candidates, frequent failures. *Alzheimer's Res. Ther.* 6, 37. <https://doi.org/10.1186/alzrt269>.

Eroglu, C., and Barres, B.A. (2010). Regulation of synaptic connectivity by glia. *Nature* 468, 223–231. <https://doi.org/10.1038/nature09612>.

Falk, A., Koch, P., Kesavan, J., Takashima, Y., Ladewig, J., Alexander, M., Wiskow, O., Tailor, J., Trotter, M., Pollard, S., et al. (2012). Capture of neuroepithelial-like stem cells from pluripotent stem cells provides a versatile system for in vitro production of human neurons. *PLoS One* 7, e29597. <https://doi.org/10.1371/journal.pone.0029597>.

Fenske, P., Grauel, M.K., Brockmann, M.M., Dorn, A.L., Trimbuch, T., and Rosenmund, C. (2019). Autaptic cultures of human induced neurons as a versatile platform for studying synaptic function and neuronal morphology. *Sci. Rep.* 9, 4890. <https://doi.org/10.1038/s41598-019-41259-1>.

Hama, H., Hara, C., Yamaguchi, K., and Miyawaki, A. (2004). PKC signaling mediates global enhancement of excitatory synaptogenesis in neurons triggered by local contact with astrocytes. *Neuron* 41, 405–415. [https://doi.org/10.1016/s0896-6273\(04\)00007-8](https://doi.org/10.1016/s0896-6273(04)00007-8).

Hedegaard, A., Monzón-Sandoval, J., Newey, S.E., Whiteley, E.S., Webber, C., and Akerman, C.J. (2020). Pro-maturational effects of human iPSC-derived cortical astrocytes upon iPSC-derived cortical neurons. *Stem Cell Rep.* 15, 38–51. <https://doi.org/10.1016/j.stemcr.2020.05.003>.

Hessler, N.A., Shirke, A.M., and Malinow, R. (1993). The probability of transmitter release at a mammalian central synapse. *Nature* 366, 569–572. <https://doi.org/10.1038/366569a0>.

Huettnner, J.E., and Baughman, R.W. (1986). Primary culture of identified neurons from the visual cortex of postnatal rats. *J. Neurosci.* 6, 3044–3060. <https://doi.org/10.1523/JNEUROSCI.06-10-03044.1986>.

Katsurabayashi, S., Oyabu, K., Kubota, K., Watanabe, T., Nagamatsu, T., Akaike, N., and Iwasaki, K. (2021). The novel mitochondria activator, 10-ethyl-3-methylpyrimido[4, 5-b]quinoline-2, 4(3H, 10H)-dione (TND128), promotes the development of hippocampal neuronal morphology. *Biochem. Biophys. Res. Commun.* 560, 146–151. <https://doi.org/10.1016/j.bbrc.2021.04.132>.

Kawano, H., Katsurabayashi, S., Kakazu, Y., Yamashita, Y., Kubo, N., Kubo, M., Okuda, H., Takasaki, K., Kubota, K., Mishima, K., et al. (2012). Long-term culture of astrocytes attenuates the readily releasable pool of synaptic vesicles. *PLoS One* 7, e48034. <https://doi.org/10.1371/journal.pone.0048034>.

Kawano, H., Oyabu, K., Yamamoto, H., Eto, K., Adaniya, Y., Kubota, K., Watanabe, T., Hirano-Iwata, A., Nabekura, J., Katsurabayashi, S., and Iwasaki, K. (2017). Astrocytes with previous chronic exposure to amyloid β -peptide fragment 1-40 suppress excitatory synaptic transmission. *J. Neurochem.* 143, 624–634. <https://doi.org/10.1111/jnc.14247>.

Leventoux, N., Morimoto, S., Imaizumi, K., Sato, Y., Takahashi, S., Mashima, K., Ishikawa, M., Sonn, I., Kondo, T., Watanabe, H., and Okano, H. (2020). Human astrocytes model derived from induced pluripotent stem cells. *Cells* 9, 2680. <https://doi.org/10.3390/cells9122680>.

Lischka, F.W., Efthymiou, A., Zhou, Q., Nieves, M.D., McCormack, N.M., Wilkerson, M.D., Sukumar, G., Dalgard, C.L., and Doughty, M.L. (2018). Neonatal mouse cortical but not isogenic human astrocyte feeder layers enhance the functional maturation of induced pluripotent stem cell-derived neurons in culture. *Glia* 66, 725–748. <https://doi.org/10.1002/glia.23278>.

Lundin, A., Delsing, L., Clausen, M., Ricchiuto, P., Sanchez, J., Sabirsh, A., Ding, M., Synnergren, J., Zetterberg, H., Brolén, G., et al. (2018). Human iPSC-derived astroglia from a stable neural precursor state show improved functionality compared with conventional astrocytic models. *Stem Cell Rep.* 10, 1030–1045. <https://doi.org/10.1016/j.stemcr.2018.01.021>.

McCarthy, K.D., and de Vellis, J. (1980). Preparation of separate astroglial and oligodendroglial cell cultures from rat cerebral tissue. *J. Cell. Biol.* 85, 890–902. <https://doi.org/10.1083/jcb.85.3.890>.

Meijer, M., Rehbach, K., Brunner, J.W., Classen, J.A., Lammertse, H.C.A., van Linge, L.A., Schut, D., Krutenko, T., Hebisch, M., Cornelisse, L.N., et al. (2019). A single-cell model for synaptic transmission and plasticity in human iPSC-derived neurons. *Cell Rep.* 27, 2199–2211.e6. <https://doi.org/10.1016/j.celrep.2019.04.058>.

Oberheim, N.A., Takano, T., Han, X., He, W., Lin, J.H.C., Wang, F., Xu, Q., Wyatt, J.D., Pilcher, W., Ojemann, J.G., et al. (2009). Uniquely hominid features of adult human astrocytes. *J. Neurosci.* 29, 3276–3287. <https://doi.org/10.1523/JNEUROSCI.4707-08.2009>.

Oberheim, N.A., Wang, X., Goldman, S., and Nedergaard, M. (2006). Astrocytic complexity distinguishes the human brain. *Trends Neurosci.* 29, 547–553. <https://doi.org/10.1016/j.tins.2006.08.004>.

Oyabu, K., Kiyota, H., Kubota, K., Watanabe, T., Katsurabayashi, S., and Iwasaki, K. (2019). Hippocampal neurons in direct contact with astrocytes exposed to amyloid β 25-35 exhibit reduced excitatory synaptic transmission. *IBRO Rep.* 7, 34–41. <https://doi.org/10.1016/j.ibro.2019.07.1719>.

Oyabu, K., Takeda, K., Kawano, H., Kubota, K., Watanabe, T., Harata, N.C., Katsurabayashi, S., and Iwasaki, K. (2020). Presynaptically silent synapses are modulated by the density of surrounding astrocytes. *J. Pharm. Sci.* 144, 76–82. <https://doi.org/10.1016/j.jphs.2020.07.009>.

Patel, D.C., Tewari, B.P., Chaunsali, L., and Sontheimer, H. (2019). Neuron-glia interactions in the pathophysiology of epilepsy. *Nat. Rev. Neurosci.* 20, 282–297. <https://doi.org/10.1038/s41583-019-0126-4>.

Perea, G., Navarrete, M., and Araque, A. (2009). Tripartite synapses: astrocytes process and control synaptic information. *Trends Neurosci.* 32, 421–431. <https://doi.org/10.1016/j.tins.2009.05.001>.

Perriot, S., Mathias, A., Perriard, G., Canales, M., Jonkmans, N., Merienne, N., Meunier, C., El Kassar, L., Perrier, A.L., Laplaud, D.A., et al. (2018). Human induced pluripotent stem cell-derived astrocytes are differentially activated by multiple sclerosis-associated cytokines. *Stem Cell Rep.* 11, 1199–1210. <https://doi.org/10.1016/j.stemcr.2018.09.015>.

- Petrelli, F., Pucci, L., and Bezzi, P. (2016). Astrocytes and microglia and their potential link with autism spectrum disorders. *Front. Cell. Neurosci.* 10, 21. <https://doi.org/10.3389/fncel.2016.00021>.
- Pyott, S.J., and Rosenmund, C. (2002). The effects of temperature on vesicular supply and release in autaptic cultures of rat and mouse hippocampal neurons. *J. Physiol.* 539, 523–535. <https://doi.org/10.1113/jphysiol.2001.013277>.
- Rhee, H.J., Shaib, A.H., Rehbach, K., Lee, C., Seif, P., Thomas, C., Gideons, E., Guenther, A., Krutenko, T., Hebisch, M., et al. (2019). An autaptic culture system for standardized analyses of iPSC-derived human neurons. *Cell Rep.* 27, 2212–2228.e7. <https://doi.org/10.1016/j.celrep.2019.04.059>.
- Rosenmund, C., Clements, J.D., and Westbrook, G.L. (1993). Nonuniform probability of glutamate release at a hippocampal synapse. *Science* 262, 754–757. <https://doi.org/10.1126/science.7901909>.
- Rothstein, J.D. (2003). Of mice and men: reconciling preclinical ALS mouse studies and human clinical trials. *Ann. Neurol.* 53, 423–426. <https://doi.org/10.1002/ana.10561>. PMID: 12666108.
- Roybon, L., Lamas, N.J., Garcia, A.D., Yang, E.J., Sattler, R., Lewis, V.J., Kim, Y.A., Kachel, C.A., Rothstein, J.D., Przedborski, S., et al. (2013). Human stem cell-derived spinal cord astrocytes with defined mature or reactive phenotypes. *Cell Rep.* 4, 1035–1048. <https://doi.org/10.1016/j.celrep.2013.06.021>.
- Russo, F.B., Freitas, B.C., Pignatari, G.C., Fernandes, I.R., Sebat, J., Muotri, A.R., and Beltrão-Braga, P.C.B. (2018). Modeling the interplay between neurons and astrocytes in autism using human induced pluripotent stem cells. *Biol. Psychiatry.* 83, 569–578. <https://doi.org/10.1016/j.biopsych.2017.09.021>.
- Santos, R., Vadodaria, K.C., Jaeger, B.N., Mei, A., Lefcochilos-Fogelquist, S., Mendes, A.P.D., Erikson, G., Shokhirev, M., Randolph-Moore, L., Fredlender, C., et al. (2017). Differentiation of inflammation-responsive astrocytes from glial progenitors generated from human induced pluripotent stem cells. *Stem Cell Rep.* 8, 1757–1769. <https://doi.org/10.1016/j.stemcr.2017.05.011>.
- Suga, M., Kondo, T., and Inoue, H. (2019). Modeling neurological disorders with human pluripotent stem cell-derived astrocytes. *Int. J. Mol. Sci.* 20, 3862. <https://doi.org/10.3390/ijms20163862>.
- Takahashi, K., Tanabe, K., Ohnuki, M., Narita, M., Ichisaka, T., Tomoda, K., and Yamanaka, S. (2007). Induction of pluripotent stem cells from adult human fibroblasts by defined factor. *Cell* 131, 861–872.
- Takeda, K., Watanabe, T., Oyabu, K., Tsukamoto, S., Oba, Y., Nakano, T., Kubota, K., Katsurabayashi, S., and Iwasaki, K. (2021). Valproic acid-exposed astrocytes impair inhibitory synapse formation and function. *Sci. Rep.* 11, 23. <https://doi.org/10.1038/s41598-020-79520-7>.
- Tchieu, J., Calder, E.L., Guttikonda, S.R., Gutzwiller, E.M., Aromolaran, K.A., Steinbeck, J.A., Goldstein, P.A., and Studer, L. (2019). NFIA is a gliogenic switch enabling rapid derivation of functional human astrocytes from pluripotent stem cells. *Nat. Biotechnol.* 37, 267–275. <https://doi.org/10.1038/s41587-019-0035-0>.
- Tcw, J., Wang, M., Pimenova, A.A., Bowles, K.R., Hartley, B.J., Lacin, E., Machlovi, S.I., Abdelaal, R., Karch, C.M., Phatnani, H., et al. (2017). An efficient platform for astrocyte differentiation from human induced pluripotent stem cells. *Stem Cell Rep.* 9, 600–614. <https://doi.org/10.1016/j.stemcr.2017.06.018>.
- Uchino, K., Kawano, H., Tanaka, Y., Adaniya, Y., Asahara, A., Deshimaru, M., Kubota, K., Watanabe, T., Katsurabayashi, S., Iwasaki, K., and Hirose, S. (2021). Inhibitory synaptic transmission is impaired at higher extracellular Ca²⁺ concentrations in Scn1a^{+/-} mouse model of Dravet syndrome. *Sci. Rep.* 11, 10634. <https://doi.org/10.1038/s41598-021-90224-4>.
- VanderWall, K.B., Vij, R., Ohlemacher, S.K., Sridhar, A., Fligor, C.M., Feder, E.M., Edler, M.C., Baucum, A.J., 2nd, Cummins, T.R., and Meyer, J.S. (2019). Astrocytes regulate the development and maturation of retinal ganglion cells derived from human pluripotent stem cells. *Stem Cell Rep.* 12, 201–212. <https://doi.org/10.1016/j.stemcr.2018.12.010>.
- Waldmeier, P., Bozyczko-Coyne, D., Williams, M., and Vaught, J.L. (2006). Recent clinical failures in Parkinson's disease with apoptosis inhibitors underline the need for a paradigm shift in drug discovery for neurodegenerative diseases. *Biochem. Pharmacol.* 72, 1197–1206. <https://doi.org/10.1016/j.bcp.2006.06.031>.
- Williams, E.C., Zhong, X., Mohamed, A., Li, R., Liu, Y., Dong, Q., Ananiev, G.E., Mok, J.C.C., Lin, B.R., Lu, J., et al. (2014). Mutant astrocytes differentiated from Rett syndrome patients-specific iPSCs have adverse effects on wild-type neurons. *Hum. Mol. Genet.* 23, 2968–2980. <https://doi.org/10.1093/hmg/ddu008>.
- Zamanian, J.L., Xu, L., Foo, L.C., Nouri, N., Zhou, L., Giffard, R.G., and Barres, B.A. (2012). Genomic analysis of reactive astrogliosis. *J. Neurosci.* 32, 6391–6410. <https://doi.org/10.1523/JNEUROSCI.6221-11.2012>.
- Zhang, Y., Sloan, S.A., Clarke, L.E., Caneda, C., Plaza, C.A., Blumenthal, P.D., Vogel, H., Steinberg, G.K., Edwards, M.S.B., Li, G., et al. (2016). Purification and characterization of progenitor and mature human astrocytes reveals transcriptional and functional differences with mouse. *Neuron* 89, 37–53. <https://doi.org/10.1016/j.neuron.2015.11.013>.

STAR★METHODS

KEY RESOURCES TABLE

REAGENT or RESOURCE	SOURCE	IDENTIFIER
Antibodies		
Mouse anti-Nestin monoclonal antibody	Abcam	Cat# ab22035, RRID: AB_446723
DACH1 rabbit polyclonal antibody	Proteintech	Cat# 10914-1-AP
Mouse anti-GFAP monoclonal antibody	Sigma-Aldrich	Cat# G3893, RRID: AB_477010
Rabbit anti-S100 β monoclonal antibody	Abcam	Cat# ab52642, RRID: AB_882426
Guinea pig anti-MAP2 polyclonal antibody	Synaptic Systems	Cat# 188 004
Rabbit anti-VGLUT1 polyclonal antibody	Synaptic Systems	Cat# 135 303 RRID: AB_2744597
Rabbit anti-GFAP polyclonal antibody	Synaptic Systems	Cat# 173 002 RRID: AB_2864794
Chemicals, peptides, and recombinant proteins		
Alexa Fluor 555 mouse	Thermo Fisher Scientific	Cat# A32727
Alexa Fluor 488 rabbit	Thermo Fisher Scientific	Cat# A32731
Alexa Fluor 488 guinea pig	Thermo Fisher Scientific	Cat# A-11073
Alexa Fluor 594 rabbit	Thermo Fisher Scientific	Cat# A32740
iMatrix-511	Takara Bio	Cat# 892011
StemFit AK02N	Ajinomoto	Cat# AK02N
Animal-Free Recombinant Human EGF	PeproTech	Cat# AF-100-15
FGF-basic(154a.a.), Human, Recombinant	PeproTech	Cat# 100-18B
Matrigel	Corning	Cat# 356230
human LIF	Sigma-Aldrich	Cat# LIF1010
B-27™ Supplement (50X), minus vitamin A	Thermo Fischer Scientific	Cat# 12587010
CNTF	PeproTech	Cat# AF-450-13
MITO+ Serum Extender	Corning	Cat# 355006
mitomycin C	Nacalai Tesque,	Cat# 20898-21
Collagen	Corning	Cat# 354236
poly-D-lysine	Sigma-Aldrich	Cat# P6407-5MG
Papain	Worthington	Cat# PAP
B-27™ Supplement (50X), serum free	Thermo Fischer Scientific	Cat# 17504044
Hoechst 33258	Sigma-Aldrich	Cat# B2261
Experimental models: Organisms/strains		
Jcl:ICR	CLEA	N/A
Oligonucleotides		
β -actin primer forward: GATCAAGATCATTGCTCCTCCT	Sigma-Aldrich	N/A
β -actin primer reverse: GGGTGTAACGCAACTAAGTCA	Sigma-Aldrich	N/A
Gfap primer forward: ACATCGAGATCGCCACCTAC	Sigma-Aldrich	N/A
Gfap primer reverse: CGGAGCAACTATCCTGCTTC	Sigma-Aldrich	N/A
CD44 primer forward: CTGCCGCTTGCAGGTGTA	Sigma-Aldrich	N/A
CD44 primer reverse: CATTGTGGGCAAGGTGCTATT	Sigma-Aldrich	N/A

(Continued on next page)

Continued

REAGENT or RESOURCE	SOURCE	IDENTIFIER
SOX1 primer forward: GAAATAGCCAATGCCAGGTG,	Sigma-Aldrich	N/A
SOX1 primer reverse: CCGTGAATACGATGAGTGTACC	Sigma-Aldrich	N/A

RESOURCE AVAILABILITY**Lead contact**

Further information and requests for resources and reagents should be directed to and will be fulfilled by the lead contact, Shutaro Katsurabayashi (shutarok@fukuoka-u.ac.jp).

Materials availability

This study did not generate new unique reagents.

Data and code availability

- All data reported in this paper will be shared by the [lead contact](#) upon request.
- This paper does not report original code.
- Any additional information required to reanalyze the data reported in this paper is available from the [lead contact](#) upon request.

EXPERIMENTAL MODEL AND SUBJECT DETAILS**Animals**

Experimental animals were handled under the ethical regulations for animal experiments of the Fukuoka University experimental animal care and use committee and animal experiment implementation. All animal protocols were approved by the ethics committee of Fukuoka University (permit number: 1912103). Pregnant ICR mice for the neuron cultures were purchased from CLEA Japan, Inc. (catalog ID: Jcl:ICR). Mice were individually housed in plastic cages and kept in an animal house under the following conditions: room temperature 23°C ± 2°C, humidity 60% ± 2%, and a 12-hour light/dark cycle (7:00 AM lights on), with free access to water and food (CE-2, Nihon Crea).

iPSC line

Research using human iPS cells was conducted in accordance with the "Guidelines for Clinical Research Using Human Stem Cells (MHLW, Japan)", and in a manner that was discussed and approved by the Fukuoka University "Medical Ethics Committee (approval number 418)".

METHOD DETAILS**Establishing and maintaining Lt-NES cells derived from 201B7 iPSCs**

The iPSC line 201B7 was established and maintained as previously described ([Takahashi et al., 2007](#)). 201B7 iPSCs were cultured in iMatrix-511-coated (892011; Takara Bio, Kusatsu, Japan) dishes containing StemFit AK02N medium (Ajinomoto, Tokyo, Japan). Lt-NES cells were established from the 201B7 iPSCs as previously described ([Falk et al., 2012](#)). Lt-NES cells derived from 201B7 iPSCs were maintained in N2 media supplemented with 10 ng/mL epidermal growth factor (EGF; PeproTech, Rocky Hill, NJ) and 10 ng/mL basic fibroblast growth factor (bFGF; StemCultures, Rensselaer, NY) as previously described ([Falk et al., 2012](#)). iPSC-derived NPC cultures were maintained in N2 media supplemented with 10 ng/mL EGF (PeproTech) and 10 ng/mL bFGF (StemCultures) as previously described ([Falk et al., 2012](#)).

Generation of HiAs

We differentiated HiAs as previously reported ([Perriot et al., 2018](#)). Lt-NES cells were dissociated with trypsin-EDTA, plated on Matrigel (Corning, Corning, NY)-coated T25-flask at 1 × 10⁶ cells in Astrocyte Induction Medium (DMEM/F12; Sigma-Aldrich, St Louis, USA, GlutaMax; Thermo Fisher Scientific, Waltham, MA, 1/100, N2 supplement; Thermo Fisher Scientific, 1/100, 10 ng/ml LIF; Sigma-Aldrich, 10 ng/ml EGF; PeproTech, B27 minus vitamin A; Thermo Fischer Scientific, 1/50) and medium was changed every 3–4 days for 2 weeks. After 2 weeks, cells were trypsinized, and a half volume of cells was plated on

Matrigel-coated T25-flasks in Astrocyte Maturation Medium (DMEM/F12, GlutaMax 1/100, B27 minus vitamin A 1/50, 20 ng/ml CNTF; PeproTech) and incubated for 4 weeks, changing the medium every 3 to 4 days. Four weeks later, the cells were removed by trypsin and plated in Matrigel-coated T75 flasks in 10% FBS/DMEM (DMEM, FBS 1/10, GlutaMax 1/100, MITO+ Serum Extender; Corning, 1/1000) and incubated for a week. Finally, the cells were reacted with mitomycin C (Nacalai Tesque, Kyoto, Japan) in 10 μ g/ml for 2 hours to inhibit cell proliferation. For cryopreservation, cells were trypsinized, and around $1-2 \times 10^6$ cells were spun down and resuspended in CELLBANKER 2 before freezing at -80°C .

HiAAs and NMCs

For the culturing of HiAs as microislands, 22-mm coverslips were pre-coated uniformly with 0.5% liquefied agarose to prevent cells from attaching. The next day or later, a mixture of collagen (final concentration of 1 mg/ml, BD Biosciences, Franklin Lakes, NJ) and poly-D-lysine (final concentration 0.5 mg/ml, Sigma-Aldrich) was applied on top of the agarose layer, using a custom-made dot-stamp designed to deposit substrate in 300- μ m squares. Cryopreserved HiAs were quickly thawed in a 37°C water bath and transferred to a 15 ml tube. Then, 5 ml pre-warmed 10% FBS/DMEM was slowly added and cells were spun down. Cells were resuspended with 10% FBS/DMEM and viable cells were counted. HiAs were plated on the dot-stamped coverslips prepared for microisland culture at a density of 25×10^3 cells/well and incubated in 10% FBS/DMEM for approximately one week. After the astrocytes formed microislands, we co-cultured them with mouse primary hippocampal neurons. Hippocampi (CA3–CA1 regions) were isolated from the brains of newborn ICR mice from both sex, and enzymatically dissociated in DMEM containing papain (2 units/mL, Worthington, Lakewood, NJ), for 60 min at 37°C . The cells were plated at a density of 6,000 cells/well onto the HiAs microislands. Before the dissociated hippocampal neurons were plated, the medium was replaced with Neurobasal-A-medium (NBM; Thermo Fisher Scientific, B27; Thermo Fisher Scientific, 1/50, GlutaMax 1/100, penicillin-streptomycin 1/100). For NMCs, hippocampal neurons were plated at a density of 6,000 cells/well in NBM onto glass coverslips coated in the same way as for the microislands. To maintain the soluble factor in HiAAs and NMCs, the medium was not changed during the culture period.

Quantitative PCR

Real-time RT-PCR analysis was performed according to the procedures described (Takeda et al., 2021). Total RNA was extracted from cultured HiAs and Lt-NES cells using RLT lysis buffer (Qiagen, Venlo, Nederland). Quantitative PCR was conducted on a LightCycler Nano System (Roche Diagnostics, Mannheim, Germany). Primers were as follows: *β -actin*, forward: GATCAAGATCATTGCTCCTCCT, reverse: GGGTGTAAACG CAACTAAGTCA; *Gfap*, forward: ACATCGAGATCGCCACCTAC, reverse: CGGAGCAACTATCCTGCTTC; *CD44*, forward: CTGCCGCTTTGCAGGTGTA, reverse: CATTGTGGCAAGGTGCTATT; *SOX1*, forward: GAAATAGCCAATGCCAGGTG, reverse: CCGTGAATACGATGAGTGTTACC. Analysis of PCR data was performed using the comparative Ct method.

Purity of HiAs

HiAs were plated in Matrigel-coated 22-mm coverslips at a density of 6×10^4 cells/well and incubated in 10% FBS/DMEM for approximately one week. HiAs cultured on coverslips were fixed in 4% paraformaldehyde in phosphate-buffered saline for 20 min. They were then incubated with anti-GFAP antibodies (rabbit polyclonal, Synaptic Systems, Gottingen, Germany, 1:1000 dilution) in blocking solution (0.1% Triton X-100, 2% normal goat serum) at 4°C overnight. Next, the cells were incubated in Alexa Fluor 594 (1:400, Thermo Fisher Scientific) for 40 min at room temperature. The nuclei of astrocytes were visualized by counterstaining with 4',6-diamidino-2-phenylindole (DAPI)-containing mounting medium (ProLong® Gold Antifade Reagent with DAPI, Thermo Fisher Scientific). The numbers of GFAP positively stained cells in square areas were counted twice, independently per culture batch, and their percentage was calculated. Data were obtained from seven cultures.

Immunocytochemistry, image acquisition, and analysis

Lt-NES cells were fixed with 4% PFA, permeabilized with 0.2% Triton X-100, and blocked with 5% FBS in PBS, before incubation with primary antibodies against the neuronal progenitor marker Nestin (diluted 1:200; Abcam, Cambridge, UK, ab22035) and the neuronal rosette maker DACH1 (diluted 1:200; Proteintech, 10914-1-AP).

Astrocytes derived from Lt-NES cells were fixed with 4% PFA, permeabilized with 0.2% Triton X-100, and blocked with 5% FBS in PBS, before incubation with primary antibodies against the astrocyte markers GFAP (diluted 1:400; Sigma-Aldrich, G3893) and S100 β (diluted 1:200; Abcam, ab52642). They were then washed with PBS at room temperature and incubated with Alexa Fluor 488- or 555-conjugated secondary antibodies (diluted 1:1000; Thermo Fisher Scientific,). Nuclei were stained with Hoechst 33258 (1:1000, B2261; Sigma-Aldrich), and images were recorded using a fluorescence microscope (BZ-X700; Keyence, Osaka, Japan).

Neurons and astrocytes were fixed in 4% paraformaldehyde in phosphate-buffered saline for 20 min. They were then incubated with primary antibodies containing blocking solution (0.1% Triton X-100, 2% normal goat serum) at 4°C overnight. The following primary antibodies were used: anti-MAP2 (guinea-pig polyclonal, antiserum, 1:1000 dilution, Synaptic Systems), anti-VGLUT1 rabbit polyclonal, affinity purified, Synaptic Systems, 1:2000 dilution), and anti-GFAP (rabbit polyclonal, Synaptic Systems, 1:1000 dilution). Next, the cells were incubated with secondary antibodies corresponding to each primary antibody (Alexa Fluor 488 for MAP2, Alexa Fluor 594 for VGLUT1 and GFAP, both 1:400, Thermo Fisher Scientific) for 40 min at room temperature. The nuclei of astrocytes and autaptic neurons were visualized by counterstaining with DAPI-containing mounting medium.

Confocal images of neurons were captured as previously reported (Kawano et al., 2012). Synaptic puncta were analyzed as previously reported (Oyabu et al., 2019). Dendritic morphologies were analyzed as previously reported (Takeda et al., 2021).

Electrophysiology

All electrophysiological experiments were performed using the patch-clamp method, where the membrane potential was clamped at -70 mV. Evoked EPSCs and depolarization-induced Na⁺ currents were recorded in response to an action potential elicited by a brief (2 ms) somatic depolarization pulse (to 0 mV) from the patch pipette under voltage-clamp conditions. Spontaneous mEPSCs were recorded in the presence of an Na⁺ channel inhibitor, 0.5 μ M tetrodotoxin (Fujifilm Wako Pure Chemical Corporation, Osaka, Japan), in the extracellular fluid. Synaptic responses were recorded at a sampling rate of 20 kHz and were filtered at 10 kHz. Data were excluded from the analysis if a leak current >300 pA was observed. The data were analyzed offline using AxoGraph X 1.2 software (AxoGraph Scientific).

Extracellular fluid (pH 7.4) was as follows (mM): NaCl 140, KCl 2.4, HEPES 10, glucose 10, CaCl₂ 2, and MgCl₂ 1. Some experiments were performed under Mg²⁺-free/10 μ M glycine conditions. In these cases, the composition of the extracellular solution was modified only with regard to Mg²⁺ and glycine without readjusting the concentration of the other ions. Intracellular fluid (pH 7.4) was as follows (mM): K-gluconate 146.3, MgCl₂ 0.6, ATP-Na₂ 4, GTP-Na₂ 0.3, creatine phosphokinase 50 U/mL, phosphocreatine 12, EGTA 1, and HEPES 17.8.

QUANTIFICATION AND STATISTICAL ANALYSIS

Statistical analysis

All statistical tests were performed using KaleidaGraph software. To compare two groups, we used an unpaired Student's *t*-test, and for multiple comparisons, we used Tukey's test. The results are expressed as the standard error of the mean (SEM). P values less than 0.05 were considered significant and are indicated as following: **p* < 0.05, ***p* < 0.01, ****p* < 0.001.